Estimation of Marine Primary Productivity From Satellite-Derived Phytoplankton Absorption Data

Sheng Ma, Zui Tao, Xiaofeng Yang, *Member*, *IEEE*, Yang Yu, Xuan Zhou, Wentao Ma, and Ziwei Li

***Abstract*—The global ocean net primary production (NPP) was estimated from satellite-derived information using a phytoplankton pigment absorption ($a_{\rm ph}$)-based model. Satellite-derived spectral-averaged $a_{\rm ph}$ was used as the key predictor of phytoplankton photosynthetic efficiency in the model. The $a_{\rm ph}$-based model yields an annual integrated NPP of approximately 55 Pg C year^{-1} for the global oceans over the period 2003–2010. The accuracy of the model was validated by comparing it with *in situ* NPP at three sites, and the logarithmic root-mean-square error of the model was approximately 0.18. The model performance was also compared with two existing NPP models (chlorophyll-based model and carbon-based model) in terms of spatial distribution, seasonal cycles, and accuracy. The comparison results indicated that the $a_{\rm ph}$-based model has improved accuracy in describing NPP variation for monthly timescales compared with the other two models. We were surprised to find that the spatial distribution of global ocean NPP provided by the $a_{\rm ph}$-based model is more similar to the carbon-based model than the chlorophyll-based model. Although many additional studies need to be conducted, the performance of the $a_{\rm ph}$-based model in this work may encourage us to estimate ocean NPP from satellite-derived phytoplankton pigment absorption.**

***Index Terms*—Net primary production (NPP), phytoplankton, pigment absorption, remote sensing.**

I. Introduction

MARINE net primary productivity (NPP) estimation plays a fundamental role in understanding global biogeochemical cycling as nearly half of global photosynthetically fixed carbon derives from ocean phytoplankton [1], [2]. Therefore, understanding the large-scale spatial and temporal dynamics of primary productivity is essential to studies of global climate processes [3]. However, traditional ship-based NPP measurements cannot provide observations over large scales and are time consuming and expensive [4], [5]. Fortunately, satellite-borne ocean color sensors routinely provide observations of various seawater biophysical variables such as chlorophyll-a concentration (Chl), phytoplankton pigment absorption ($a_{\rm ph}$), sea surface temperature (SST), and photosynthetically available radiation (*PAR*) over large areas [6]–[9]. Using these satellite-derived data in a suitable model, global NPP can be estimated quickly and efficiently.

Manuscript received September 07, 2013; revised December 17, 2013; accepted January 01, 2014. Date of publication January 28, 2014; date of current version August 21, 2014. This study was supported by Chinese Public Science and Technology Research Funds for Ocean Projects (Grant 201005009). *(Corresponding author: Z. Tao.)*

The authors are with the State Key Laboratory of Remote Sensing Science, Institute of Remote Sensing and Digital Earth, Chinese Academy of Sciences, Beijing 100101, China (e-mail: taozui8421@163.com).

W. Ma is with the College of Physical and Environmental Oceanography, Ocean University of China, Qingdao 266100, China.

Color versions of one or more of the figures in this paper are available online at http://ieeexplore.ieee.org.

Digital Object Identifier 10.1109/JSTARS.2014.2298863

In fact, many satellite-based NPP models have been proposed in recent years. Initially, simple statistical models were proposed to estimate primary production from sea surface Chl [10], [11]. These empirical algorithms are only applicable to describe production variability at annual timescales [12]. Then, more complicated NPP models were proposed by combining Chl with other remotely sensed variables. These models estimate NPP by describing the photosynthetic response of phytoplankton to light, temperature, and other environmental variables within the euphotic layer or mixed layer [13]–[20]. These models are better than empirical models in quantifying photosynthetic processes [21]–[24]. In these models, Chl is used as a major indicator of pigment biomass to estimate NPP. However, recent studies have demonstrated that variations in productivity are more related to phytoplankton absorption than to Chl [25]–[27]. Lee *et al.* also demonstrated that the absorption by phytoplankton pigments was more important for the calculation of NPP than pigment biomass [28]. Hirawake *et al.* noted that $a_{\rm ph}$ performed better than SST in representing the photosynthetic rate in the vertically generalized production model (VGPM) [29]. These field measurement works have verified the advantages of $a_{\rm ph}$ as a predictor to estimate ocean NPP.

Currently, global gridded $a_{\rm ph}$ data are operationally calculated from satellite remote sensing data using the generalized inherent optical properties (GIOP) algorithm, and improvement in the accuracy of the data has been reported by the NASA GIOP workshop [30]. The availability of operational $a_{\rm ph}$ production and previous field investigations have encouraged us to apply these satellite-derived data to estimate NPP for the global ocean. Based on the experiments of Lee *et al.* [28], this study made an attempt to apply an $a_{\rm ph}$-based model (AbPM) built from field surveys to calculate global ocean NPP from satellite-derived products. The results of this model are compared with the results derived from two other models (i.e., a Chl-based model and carbon-based model [16], [20]) to investigate the advantages and disadvantages of AbPM. The details of AbPM are discussed in Section II. Comparisons and validations of model-derived results are performed in Section III. Finally, a discussion and conclusion are provided in Section IV.

II. Methodology

A. Data

To estimate NPP, several specific input datasets were acquired. The global monthly products of *PAR*, diffuse attenuation at 490 nm ($K_{\rm d}$ (490)), euphotic zone depth ($Z_{\rm eu}$), and phytoplankton pigment absorption ($a_{\rm ph}(\lambda)$) (at 412, 443, 488, 531, 547, and 667 nm) distributed by the NASA ocean color group were

downloaded (from website: http://oceancolor.gsfc.nasa.gov/). These data were generated from the Moderate Resolution Imaging Spectroradiometer (MODIS) images for the period January 2003–December 2010. The $Z_{\rm eu}$ and $a_{\rm ph}(\lambda)$ products have a spatial resolution of 9 km, whereas the spatial resolution of other products is 18 km. Here, $Z_{\rm eu}$ was calculated using the inherent optical property (IOP)-centered approach [31] and $a_{\rm ph}(\lambda)$ was modeled with the GIOP algorithm. Nitracline depths ($z_{\rm no3}$) were calculated from monthly climatological nutrient data reported in the World Ocean Atlas and defined as the depth where $\rm nitrate + nitrite$ first exceeded $0.5\ \mu$m [32].

Approximately, 350 valid samples of $a_{\rm ph}(\lambda)$ over the 400–700 nm spectral region were downloaded from the SeaWiFS Bio-optical Archive and Storage System (SeaBASS). These field data were measured from collected water samples using the GF/F filter-pad transmission technique [27]. The *in situ* NPP data used for validation were collected from time-series programs of the Pacific [subtropical gyre station ALOHA of Hawaii Ocean Time series (HOT), California Cooperative Oceanic Fisheries Investigations (CALCOFI), and Atlantic (Bermuda Atlantic Time-series Study (BATS))]. NPP data from these three sites were based on dawn-to-dark *in situ* ^{14}C incubations from the surface to 1% light level with various depth intervals. At the three sites, NPP was measured monthly (HOT and BATS) or quarterly (CALCOFI). The trapezoidal method was applied to integrate daily NPP in the euphotic zone for all stations. The locations of all *in situ* measurement stations are shown in Fig. 1.

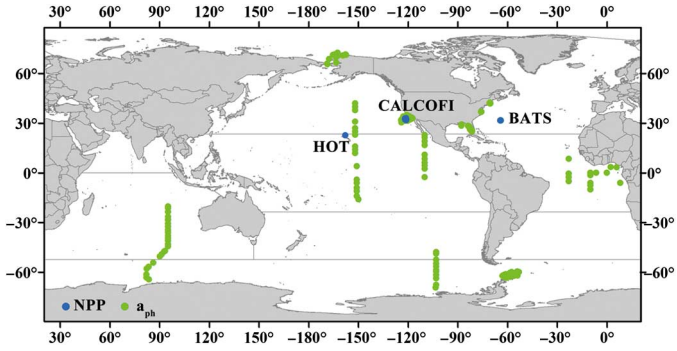

Fig. 1. Sample locations of the *in situ* NPP measurements (blue dots) and spectral phytoplankton pigment absorption data (green dots).

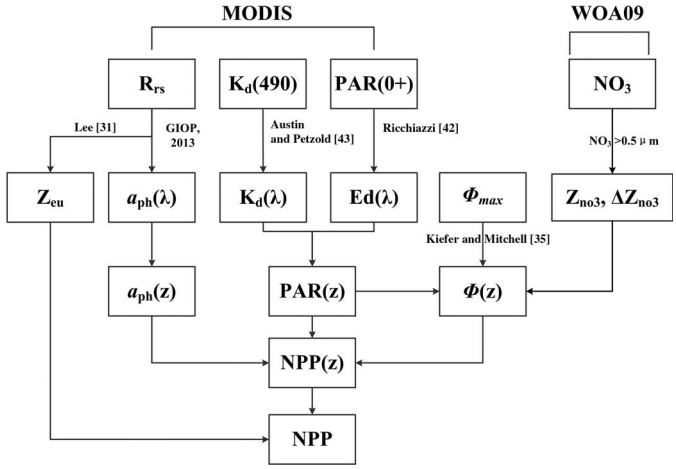

Fig. 2. Framework of the $a_{\rm ph}$-based approach for calculating ocean NPP.

B. Pigment Absorption and Primary Production Model

Fig. 2 shows the procedures of the $a_{\rm ph}$-based algorithm for estimating ocean NPP from satellite-derived *PAR*, $K_{\rm d}(490)$, $Z_{\rm eu}$, and $a_{\rm ph}(\lambda)$. The $a_{\rm ph}(\lambda)$ used in this paper is the product derived from remote sensing reflectance $\rm R_{rs}(\lambda)$ with the GIOP algorithm [30]. The GIOP algorithm is the standard algorithm for the operational $a_{\rm ph}$ products of NASA, and the products have been reported as having an approximately 20%–40% error [30]. The theoretical basis of the GIOP algorithm is briefly described by (1)–(3) as follows [30]:

$$R_{\rm rs}(\lambda) = G\frac{b_{\rm b}(\lambda)}{a(\lambda)+b_{\rm b}(\lambda)} \tag{1}$$

$$a(\lambda) = a_{\rm w}(\lambda) + a_{\rm ph}(\lambda) + a_{\rm dg}(\lambda) \tag{2}$$

$$b_{\rm b}(\lambda) = b_{\rm bw}(\lambda) + b_{\rm bp}(\lambda) \tag{3}$$

where $\rm G(sr^{-1})$ varies with the illumination conditions, $b_{\rm b}(\lambda)$ is the total backscattering coefficient $(\rm m^{-1})$, and $a(\lambda)$ is the total absorption coefficient $(\rm m^{-1})$. The subscripts w, ph, and dg indicate the absorption by water, phytoplankton, and other absorbing components (e.g., nonalgal particles and colored dissolved organic matter), respectively. The subscripts bw and bp indicate backscattering by water and particles, respectively.

According to the photosynthesis theory of phytoplankton, *NPP* at the depth z can be expressed by $a_{\rm ph}(\lambda)$ as [28], [33]

$$NPP(\rm z) = \phi(\rm z)\int_{\lambda 0}^{\lambda n} a_{\rm ph}(\lambda)E_{\rm d}(\lambda,\rm z)d\lambda \tag{4}$$

where ϕ is the quantum yield of phytoplankton photosynthesis $(\rm mol\ C\ mol\ photons^{-1})$ and $E_{\rm d}(\lambda,\rm z)$ is the quantum scalar irradiance $(\rm Ein\ m^{-2}\ nm^{-1})$ at the depth z. Equation (4) cannot be applied to satellite data directly, as $E_{\rm d}(\lambda,\rm z)$ is not a remote sensing product. However, the *PAR*, which is the integration of $E_{\rm d}(\lambda,\rm z)$ over the 400–700 nm wavelength range $(\int_{400}^{700} E_{\rm d}(\lambda,\rm z)d\lambda)$, can be derived from satellite data. Thus, a spectrally averaged absorption coefficient over 400–700 nm $(\rm m^{-1})$ $\bar{a}_{\rm ph}$ is defined as [29]

$$\bar{a}_{\rm ph}(\rm z) = \frac{\int_{400}^{700} a_{\rm ph}(\lambda)E_{\rm d}(\lambda,\rm z)d\lambda}{\int_{400}^{700} E_{\rm d}(\lambda,\rm z)d\lambda} \approx \frac{\int_{400}^{700} a_{\rm ph}(\lambda)d\lambda}{700-400}. \tag{5}$$

Then, based on the field work of Lee *et al.*, (4) is parameterized as [28]

$$NPP(\rm z) = \phi(\rm z)\times\bar{a}_{\rm ph}(\rm z)\times E(\rm z)\times\exp(-\nu\times E(\rm z)) \tag{6}$$

where ν is a photoinhibition parameter and is given by a constant of 0.01 $(\rm Ein\ m^{-1}\ day^{-1})^{-1}$ based on Platt *et al.* [34]. According to Kiefer and Mitchell [35], $\phi(z)$ in (6) is expressed as

$$\phi(\rm z) = \frac{K_{\rm m}}{K_{\rm m}+E(\rm z)}\phi_{\max} \tag{7}$$

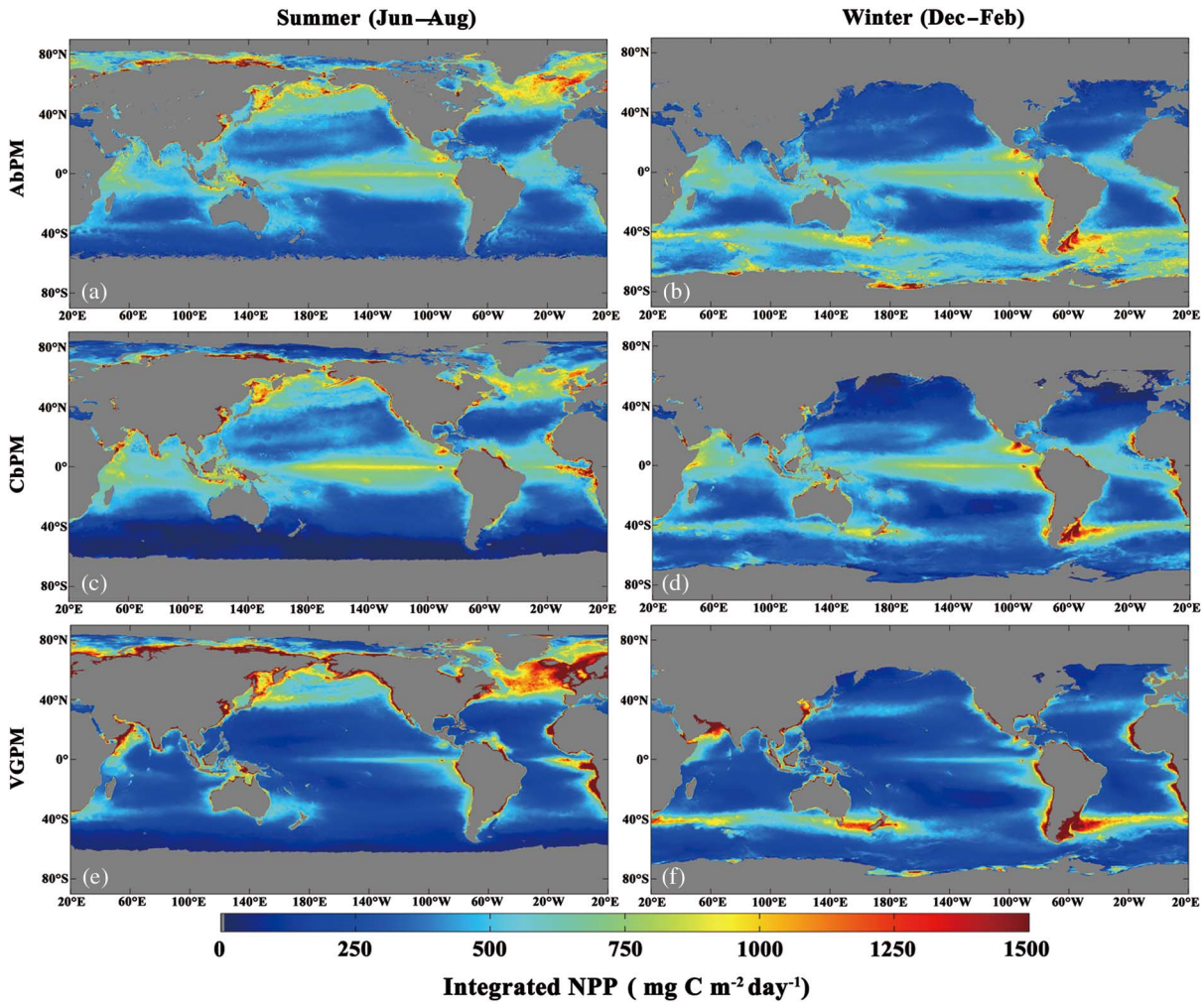

Fig. 3. Depth-integrated NPP (mg C m^{-2} day^{-1}) from three models (AbPM, CbPM, and VGPM) for the boreal summer and winter. Values are climatological means calculated for periods from 2003 to 2010.

where $\phi_{\max}$ is the value for maximum quantum yield. K_m is the irradiance when $\phi(z) = 0.5\phi_{\max}$ and is typically given as 10 Ein day^{-1} [35]. Theoretically, $\phi_{\max}$ can reach 0.125 mol C(mol photons)$^{-1}$. However, nonperfect energy transfer and limited nitrogen source assimilation typically make it less than 0.08 mol C (mol photons)$^{-1}$ [36]–[38]. According to Cleveland *et al.* [39]–[41], it has been widely accepted that $\phi_{\max}$ increases with decreasing nitrogen stress. $\phi_{\max}$ is defined as follows using the Nitracline depths z_{no3} to roughly describe the variability in depth:

$$\phi_{\max} = \begin{cases} 0.03, & \mathrm{z} < \mathrm{z_{no3}} \\ 0.03 + 0.05 \times (1 - \exp(-0.025 \times (\mathrm{z} - \mathrm{z_{no3}}))), & \mathrm{z} \geq \mathrm{z_{no3}}. \end{cases} \tag{8}$$

The integration of irradiance $E(z)$ in (6) can be calculated [20] as follows:

$$E(\mathrm{z}) = PAR(\mathrm{z}) = \int_{400}^{700} E_{\mathrm{d}}(\lambda, 0) \times \exp(-K_{\mathrm{d}}(\lambda) \times \mathrm{z}) d\lambda \tag{9}$$

where $E_{\mathrm{d}}(\lambda, 0)$ is the cloud-corrected surface *PAR*, which is decomposed spectrally using the method of Ricchiazzi *et al.* [42]. $K_{\mathrm{d}}(\lambda)$ was the spectral diffuse attenuation across the visible spectrum and calculated from $K_{\mathrm{d}}(490)$ using the model of Austin and Petzold [43].

C. Validation Method

The overall performance of the proposed model was evaluated in terms of both bias and variability following the method of Friedrichs *et al.* [23]. The log normalized bias (B), root-mean-square difference (RMSD), and signed unbiased RMSD (uRMSD) were calculated as follows:

$$\mathrm{B} = \overline{\log_{10}(\mathrm{NPP_m})} - \overline{\log_{10}(\mathrm{NPP_d})} \tag{10}$$

$$\mathrm{RMSD} = \left(\frac{1}{\mathrm{N}} \sum_{\mathrm{i}=1}^{\mathrm{N}} (\log_{10}(\mathrm{NPP_m(i)}) - \log_{10}(\mathrm{NPP_d(i)})) \right)^{1/2} \tag{11}$$

$$\text{signed uRMSD} = \mathrm{sign}(\sigma_{\mathrm{m}} - \sigma_{\mathrm{d}}) \times \sqrt{\mathrm{RMSD}^2 - \mathrm{B}^2} \tag{12}$$

where N is the number of samples at each site, NPP_{m} is the modeled NPP, NPP_{d} represents *in situ* data at each site, and σ_{m}

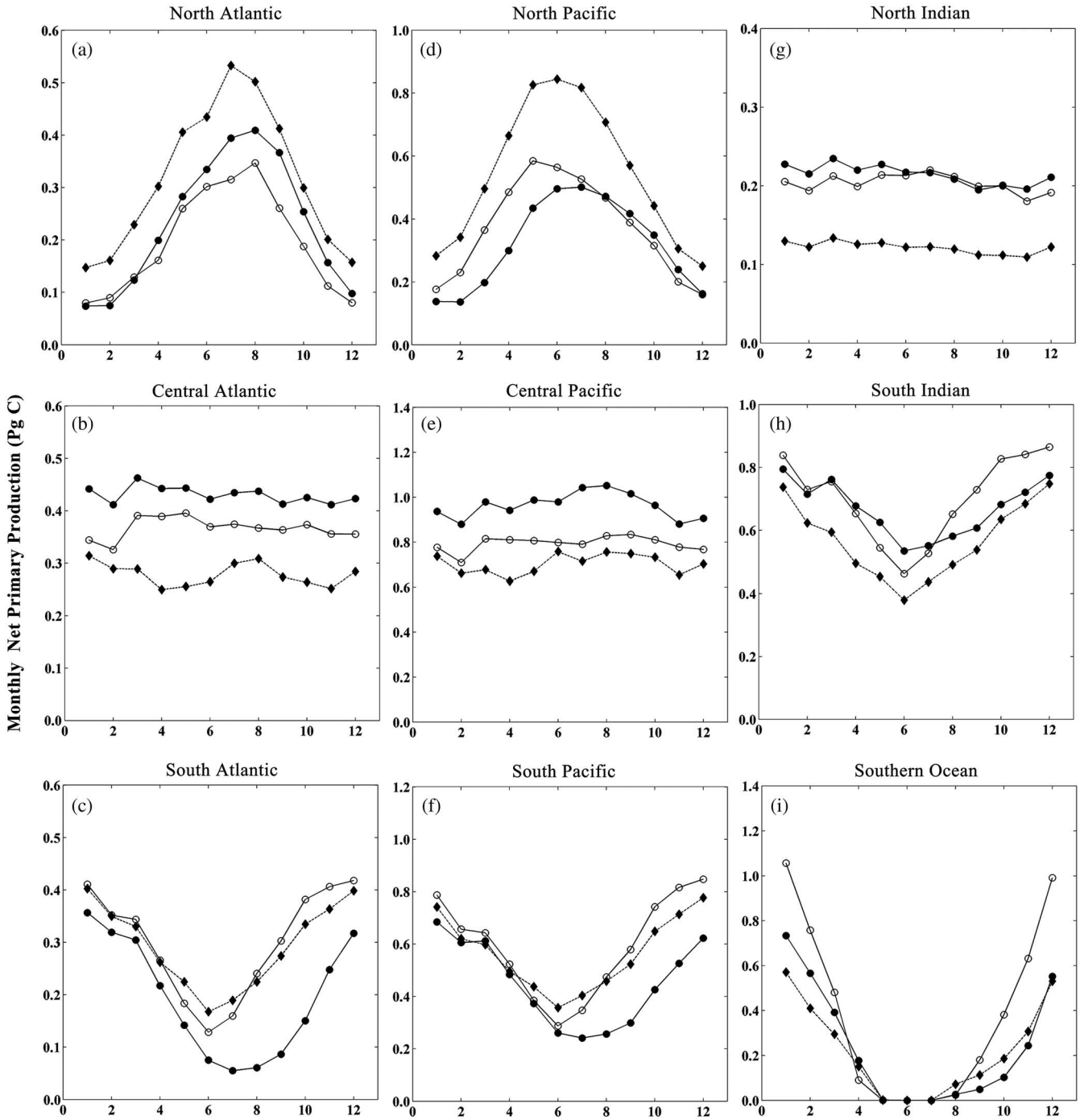

Fig. 4. Seasonal cycles in NPP for the nine ocean basins (identified in Fig. 1). Open circles denote NPP calculated from phytoplankton pigment absorption (AbPM). Solid circles denote NPP calculated from satellite phytoplankton carbon (CbPM). Solid rhombuses denote NPP calculated from chlorophyll-based model (VGPM). Seasonal cycles are based on monthly averages for the 2003–2010 period. Data were combined for all bins with each ocean basin.

and σ_{d} are the standard deviation of $\log_{10}(NPP_{\mathrm{m}})$ and $\log_{10}(NPP_{\mathrm{d}})$, respectively.

III. Results and Validation

Ocean water column productivity is the integrated values of $NPP(\mathrm{z})$ within euphotic zone (Z_{eu}). Monthly averaged *NPP* over the period from 2003 to 2010 was calculated with a $18\ \mathrm{km} \times 18\ \mathrm{km}$ spatial resolution. The boreal summer and winter depth-integrated *NPP* derived from AbPM are shown in Fig. 3(a) and (b). The maximum *NPP* values are approximately $1500\ \mathrm{mg\ C\ m^{-2}\,day^{-1}}$ and distributed mainly over the productive continental shelf areas and classical upwelling regions, such as coastal water of China, Peru, and California. Approximately a sustained $600\ \mathrm{mg\ C\ m^{-2}\,day^{-1}}$ is found throughout most of the tropic oceans. The oligotrophic gyres (lower than $300\ \mathrm{mg\ C\ m^{-2}\,day^{-1}}$) distribute to the subtropical high-pressure belt. Some small-scale heterogeneity in the

results can be traced to artifacts in nutrient products. The NPP seasonal cycles derived from the AbPM in nine ocean basins are shown in Fig. 4. The results indicated that convex or dished curves for north and south ocean basins and tiny variations in NPP were found in the tropic basins. The annual total global ocean productivity calculated by the AbPM for the period 2003–2010 is approximately 55 Pg C year^{-1} ($\text{Pg} = 10^{15}$ g), which is similar to other reported results (listed in Table I).

The NPP calculated from AbPM was compared with the results generated by two other existing models, a Chl-based model—VGPM and a carbon-based model—the updated carbon-based production model (CbPM). The annual total global ocean productivity averaged NPP values over 2003–2010 period calculated with the AbPM, VGPM, and CbPM are close to each other (55, 51, and 54 Pg C year^{-1}, respectively). However, striking spatial and seasonal differences in NPP take place in these models [shown in Fig. 3(a)–(f)]. It is interesting to note that the AbPM displayed a better agreement with CbPM than that with VGPM, especially in the northern and tropic ocean basins. Obviously, the greatest differences between the AbPM and the VGPM are in the so-called oligotrophic and eutrophic oceans, which are also reported by Marra *et al.* [44]. In the Southern Ocean (see Fig. 1 for regional boundaries), the three models displayed significant differences, particularly in the boreal winter months [shown in Fig. 3(b), (d), (f)]. In this ocean basin, the results of AbPM are 40% higher than that of CbPM and VGPM.

It is not surprising that the three models yielded different seasonal cycles in NPP as examined by ocean basin [shown in Fig. 4(a)–(i)]. For all the ocean basins, the general shape of the seasonal cycles depicted by the three models is consistent, but there are many differences in details. In the North Atlantic and North Pacific regions, the AbPM and the CbPM provided similar weaker seasonal cycles than the VGPM. In contrast, in the South Atlantic and South Pacific, the AbPM and VGPM indicated similar stronger seasonal cycles than the CbPM for July–December. In the Central Atlantic and Central Pacific, the magnitude of NPP estimated by AbPM was persistently between the values estimated by other models with no obviously seasonal variations. The AbPM kept pace with the CbPM and displayed nearly 50% higher values than the VGPM in the North Indian region. In the South Indian region, the AbPM provided almost the same values as the CbPM at the beginning of the year but displayed higher values after summer. The AbPM provided approximately 0.1–0.4 Pg C higher values than the other two models in the Southern Ocean, especially for the boreal winter.

The accuracy of the three models was validated by comparing them with the *in situ* data at three sites: HOT, BATS, and CALCOFI. The statistic parameters were calculated following (10)–(12), and the validation results are listed in Table II. Using these statistical parameters, a target diagram was plotted that allows easy visualization of whether a model over or underestimates the mean and variability of NPP (shown in Fig. 5). The target diagrams break down RMSD to show multiple statistics on a single plot: total RMSD as the distance from the origin, bias on the y-axis, and the uRMSD on the x-axis. Based on these statistical results, the overall performance of the AbPM was best among these models although it produced

TABLE I
MEAN ANNUAL GLOBAL NPP ESTIMATED FROM VARIOUS MODEL SOURCES

Models	intNPP (Pg C a^{-1})	Description
Proposed model	55	a_{ph}-based (AbPM), DR, WR
Westberry *et al.* [20]	52	C-based (CbPM), DR, WR
Behrenfeld *et al.* [18]	67	C-based (CbPM), DI, WI
Behrenfeld *et al.* [16]	44	Chl-based (VGPM), DI, WI
Carr *et al.* [4]	51	Mean of 31 global models

intNPP, depth-integrated NPP; DI, depth integrated; DR, depth resolved; WI, wavelength integrated; and WR, wavelength resolved.

TABLE II
SUMMARY STATISTICS FOR NPP MODELS AT HOT, BATS, AND CALCOFI

Location	MODEL	Bias	uRMSD	RMSD
HOT (N = 78)	AbPM	−0.06	−0.09	0.11
	VGPM	−0.31	−0.11	0.33
	CbPM	0.02	−0.12	0.12
BATS (N = 91)	AbPM	−0.14	−0.19	0.24
	VGPM	−0.16	−0.24	0.28
	CbPM	−0.22	−0.31	0.38
CALCOFI (N = 38)	AbPM	−0.02	−0.07	0.08
	VGPM	0.27	0.11	0.30
	CbPM	0.06	0.11	0.12

AbPM is the approach described in this work, CbPM refers to the carbon-based productivity model presented by Westberry *et al.* [20], VGPM refers to Behrenfeld and Falkowski's [16] vertically generalized production model. $N = 78$ for Hawaii Ocean Time-series program (HOT), $N = 91$ for Bermuda Atlantic Time-series Study (BATS), and $N = 38$ for California Cooperative Oceanic Fisheries Investigations (CALCOFI).

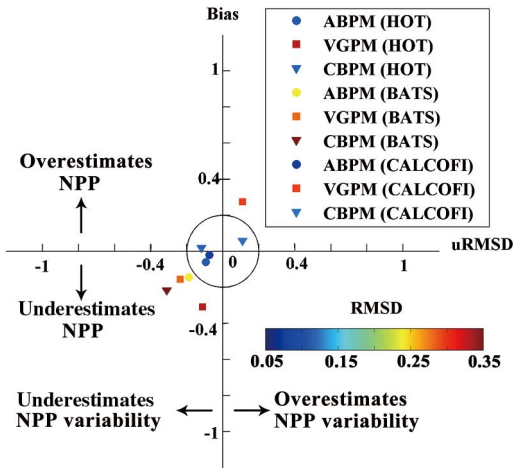

Fig. 5. Target diagrams representing model ability at HOT, BATS, and CALCOFI for three approaches. The solid circle is the averaged standard deviation of the observed data (σ_d) at the three sites. The distance from the origin to each model's symbol is the total RMSD, which was also tagged in color.

underestimations at each site (shown in Fig. 5 and Table II). The average RMSD of AbPM for all samples is as low as 0.18, which is a great improvement compared to the VGPM and CbPM at the same sites.

The NPP seasonal cycles estimated by the three models were also compared versus the *in situ* measurements at each site (shown in Fig. 6). At the HOT site, both AbPM and CbPM can

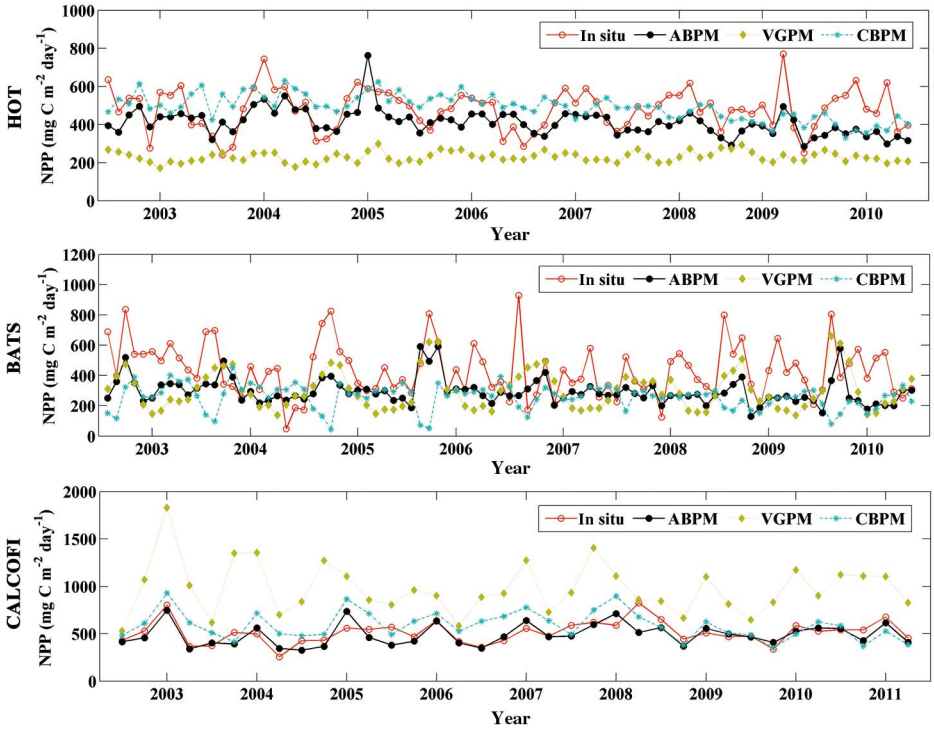

Fig. 6. Time-series comparisons of model-derived depth-integrated NPP versus *in situ* measurements of NPP at the HOT, BATS, and CALCOFI sites.

estimate the average values of NPP, whereas obvious underestimation occurs with the VGPM which has also been reported by Ondrusek *et al.* [17]. The summer blooms at the HOT station can be modeled best by the AbPM with a weaker magnitude, and it displayed the best agreement with the *in situ* data among these models in seasonal cycles. For the BATS site, seasonal differences in NPP are larger than that at HOT. None of the three models could describe the winter/spring blooms exactly. However, the AbPM and VGPM could estimate the spring blooms for the years 2003, 2005, 2006, 2009, and 2010 at BATS. The AbPM displayed the best performance in describing the seasonal cycles at the CALCOFI site among these models, and the performance of the CbPM was the second best. The VGPM at the CALCOFI site totally failed to detect the summer blooms. In general, the AbPM can best describe the seasonal variability of NPP among the three models at the sites examined in this work.

IV. Discussion and Conclusion

Our attempt to apply satellite-derived $a_{\rm ph}$ to model global ocean NPP demonstrated many improvements over two other existing models. The annual total global ocean productivity-averaged NPP calculated by the three models is close to each other. Especially for the AbPM and CbPM, similar spatial distribution of NPP displayed by them also occurs for most of the global oceans [shown in Fig. 3(a)–(d)]. These similarities imply that these models have similar performances in describing annual average value of marine NPP. However, when viewed by ocean basin, these models yield significantly different seasonal cycles in NPP. At the three sites, the AbPM performed better with seasonal cycles than the CbPM and VGPM. The results indicate that the AbPM is more sensitive in detecting NPP in seasonal cycles than the CbPM and VGPM, especially for light-limited ocean basins. For the CbPM and VGPM, photosynthesis efficiency is determined by standing biomass of phytoplankton, and the perturbations of the growth conditions in short timescales are neglected [18], whereas the AbPM can directly reflect the photosynthesis variations to the environments [27]. At the CALCOFI site, the coastal waters of California, the VGPM displayed limited success in estimating NPP. In comparison, the AbPM results were consistent with *in situ* data, which indicate the possibility of estimating NPP over coastal turbid water using an AbPM [25], [45]. Although further validation is needed, the results in this work confirm the importance of $a_{\rm ph}$ to marine NPP estimates from space. The advantages of AbPM in estimating NPP will also promote the improvement of IOP algorithms.

Nevertheless, several model components in the AbPM require further refinements and validation. For example, understanding of the influence of nutrients on maximum photosynthesis quantum yield $\phi_{\max}$ should be further studied. In this paper, a roughly simple equation based on Cleveland *et al.* was applied to describe the influence of the nutrients on $\phi_{\max}$, but this modification had a fairly limited influence on the NPP results. This type of rough descriptions of quantum yield ϕ was responsible for the major errors in the AbPM, which resulted in the overestimates in the Southern Ocean (the $\phi_{\max}$ here was reported as low as 0.01) [46], [47]. Unfortunately, the role of nutrients on maximum quantum yield remains unclear, and nearly all relevant laboratory and field studies just simplify it as a single constant [25], [28], [44]. The requirements for deriving nutrient concentrations over global ocean and modeling the influence of them on phytoplankton

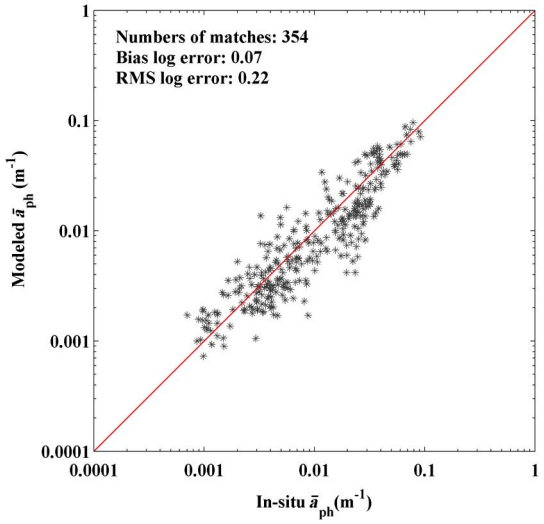

Fig. 7. Scatter plots of MODIS-derived spectral-integrated phytoplankton pigment absorption ($\bar{a}_{\rm ph}$) versus *in situ* measurements of $\bar{a}_{\rm ph}$.

photosynthesis progress also present a challenge for other satellite NPP models [18], [20]. Hence, all the models in this paper failed to detect the nutrient-dominated spring blooms at the BATS site [48]. The accuracy of satellite-derived $a_{\rm ph}(\lambda)$ is another source of the error in the NPP estimates. It is well known that the $a_{\rm ph}(\lambda)$ from satellites is an optical depth-averaged value of the upper water column ignoring the vertical variation of $a_{\rm ph}(\lambda)$, which causes errors for NPP estimates [49], [50]. In the Southern Ocean, the deviation of $a_{\rm ph}(\lambda)$ reaches higher than 50% [51], which produced great error in the AbPM. The assumption of spectrally averaged $a_{\rm ph}$ also results in errors. Compared with the *in situ* data, the mean logarithm error of the spectrally averaged $a_{\rm ph}$ is approximately 0.07 (shown in Fig. 7), which produced a nearly 10% deviation in NPP estimates. Further studies are in progress to determine the sensitivity of the AbPM to the accuracy of $a_{\rm ph}$. Another error related to $a_{\rm ph}$ is the pigment "package" effect. The satellite-derived pigment absorption is the overall absorption in the cell, including the photosynthetic pigments and nonphotosynthetic pigments [52]. The package effect refers to the decrease in absorption resulting from phytoplankton pigments being packaged within chloroplasts instead of being dissolved. Although importance of the package effect in phytoplankton photosynthetic is not clear, unanimous arguments insist that the package effect would increase with increasing size of phytoplankton and affect the accuracy of the $a_{\rm ph}$-based NPP models [44]. Therefore, the development of satellite-based approaches to obtain phytoplankton size and types may help improve the reliability of the AbPM in this work [53].

Acknowledgments

In this paper, the MODIS ocean color productions and *in situ* data of phytoplankton pigment absorption were downloaded from NASA Ocean Color websites (http://oceancolor.gsfc.nasa.gov/). The *in situ* NPP data were downloaded from the website of Hawaii Ocean Time-series program (http://hahana.soest.hawaii.edu/hot/), Bermuda Atlantic Time-series Study (http://bats.bios.edu/), and California Cooperative Oceanic Fisheries Investigations (http://www.calcofi.org/).

References

[1] M. J. Behrenfeld, J. T. Randerson, C. R. McClain, G. C. Feldman, S. O. Los, C. J. Tucker *et al.*, "Biospheric primary production during an ENSO transition," *Science*, vol. 291, no. 5513, pp. 2594–2597, Mar. 2001.

[2] P. G. Falkowski, R. T. Barber, and V. Smetacek, "Biogeochemical controls and feedbacks on ocean primary production," *Science*, vol. 281, no. 5374, pp. 200–206, Jul. 1998.

[3] A. A. Bianchi, L. Bianucci, A. R. Piola, D. R. Pino, I. Schloss, A. Poisson *et al.*, "Vertical stratification and air-sea CO_2 fluxes in the Patagonian shelf," *J. Geophys. Res.: Oceans*, vol. 110, no. C7, pp. 1–10, Jul. 2005, doi: 10.1029/2004JC002488.

[4] M. E. Carr, M. A. M. Friedrichs, M. Schmeltz, M. N. Aita, D. Antoine, K. R. Arrigo *et al.*, "A comparison of global estimates of marine primary production from ocean color," *Deep-Sea Res. II*, vol. 53, no. 5–7, pp. 741–770, 2006.

[5] S. Milutinovic and L. Bertino, "Assessment and propagation of uncertainties in input terms through an ocean-color-based model of primary productivity," *Remote Sens. Environ.*, vol. 115, no. 8, pp. 1906–1917, Aug. 2011.

[6] W. E. Esaias, M. R. Abbott, I. Barton, O. B. Brown, J. W. Campbell, K. L. Carder *et al.*, "An overview of MODIS capabilities for ocean science observations," *IEEE Trans. Geosci. Remote Sens.*, vol. 36, no. 4, pp. 1250–1265, Jul. 1998.

[7] C. R. McClain, M. L. Cleave, G. C. Feldman, W. W. Gregg, S. B. Hooker, and N. Kuring, "Science quality SeaWiFS data for global biosphere research," *Sea Technol.*, vol. 39, no. 9, pp. 10–16, Sep. 1998.

[8] R. Y. Setiawan and A. Habibi, "Satellite detection of summer chlorophyll-a bloom in the Gulf of Tomini," *IEEE J. Sel. Topics Appl. Earth Observ. Remote Sens.*, vol. 4, no. 4, pp. 944–948, Dec. 2011.

[9] R. Y. Setiawan and H. Kawamura, "Summertime phytoplankton bloom in the South Sulawesi Sea," *IEEE J. Sel. Topics Appl. Earth Observ. Remote Sens.*, vol. 4, no. 1, pp. 241–244, Mar. 2011.

[10] R. W. Eppley, E. Stewart, M. R. Abbott, and U. Heyman, "Estimating ocean primary production from satellite chlorophyll—Introduction to regional differences and statistics for the Southern-California Bight," *J. Plankton Res.*, vol. 7, no. 1, pp. 57–70, 1985.

[11] J. Campbell, D. Antoine, R. Armstrong, K. Arrigo, W. Balch, R. Barber *et al.*, "Comparison of algorithms for estimating ocean primary production from surface chlorophyll, temperature, and irradiance," *Global Biogeochem. Cycles*, vol. 16, no. 3, pp. 1–15, Jul./Aug. 2002, doi: 10.1029/2001GB001444.

[12] R. L. Iverson, W. E. Esaias, and K. Turpie, "Ocean annual phytoplankton carbon and new production, and annual export production estimated with empirical equations and CZCS data," *Global Change Biol.*, vol. 6, no. 1, pp. 57–72, Jan. 2000.

[13] T. Platt and S. Sathyendranath, "Estimators of primary production for interpretation of remotely-sensed data on ocean color," *J. Geophys. Res.: Oceans*, vol. 98, no. C8, pp. 14561–14576, Aug. 1993.

[14] A. Longhurst, S. Sathyendranath, T. Platt, and C. Caverhill, "An estimate of global primary production in the ocean from satellite radiometer data," *J. Plankton Res.*, vol. 17, no. 6, pp. 1245–1271, Jun. 1995.

[15] D. Antoine and A. Morel, "Oceanic primary production. 1. Adaptation of a spectral light-photosynthesis model in view of application to satellite chlorophyll observations," *Global Biogeochem. Cycles*, vol. 10, no. 1, pp. 43–55, Mar. 1996.

[16] M. J. Behrenfeld and P. G. Falkowski, "A consumer's guide to phytoplankton primary productivity models," *Limnol. Oceanogr.*, vol. 42, no. 7, pp. 1479–1491, Nov. 1997.

[17] M. E. Ondrusek, R. R. Bidigare, K. Waters, and D. M. Karl, "A predictive model for estimating rates of primary production in the subtropical North Pacific Ocean," *Deep-Sea Res. II*, vol. 48, no. 8–9, pp. 1837–1863, 2001.

[18] M. J. Behrenfeld, E. Boss, D. A. Siegel, and D. M. Shea, "Carbon-based ocean productivity and phytoplankton physiology from space," *Global Biogeochem. Cycles*, vol. 19, no. 1, pp. 1–14, Jan. 2005, doi: 10.1029/2004GB002299.

[19] T. Platt, S. Sathyendranath, M. H. Forget, G. N. White, C. Caverhill, H. Bouman *et al.*, "Operational estimation of primary production at large geographical scales," *Remote Sens. Environ.*, vol. 112, no. 8, pp. 3437–3448, Aug. 2008.

[20] T. Westberry, M. J. Behrenfeld, D. A. Siegel, and E. Boss, "Carbon-based primary productivity modeling with vertically resolved photoacclimation," *Global Biogeochem. Cycles*, vol. 22, no. 2, pp. 1–18, Jun. 2008, doi: 10.1029/2007GB003078.

[21] V. S. Saba, M. A. M. Friedrichs, M. E. Carr, D. Antoine, R. A. Armstrong, I. Asanuma *et al.*, "Challenges of modeling depth-integrated marine primary productivity over multiple decades: A case study at BATS and HOT," *Global Biogeochem. Cycles*, vol. 24, pp. 1–21, Sep. 2010, doi: 10.1029/2009GB003655.

[22] V. S. Saba, M. A. M. Friedrichs, D. Antoine, R. A. Armstrong, I. Asanuma, M. J. Behrenfeld *et al.*, "An evaluation of ocean color model estimates of marine primary productivity in coastal and pelagic regions across the globe," *Biogeosciences*, vol. 8, no. 2, pp. 489–503, 2011.

[23] M. A. M. Friedrichs, M. E. Carr, R. T. Barber, M. Scardi, D. Antoine, R. A. Armstrong *et al.*, "Assessing the uncertainties of model estimates of primary productivity in the tropical Pacific Ocean," *J. Mar. Sys.*, vol. 76, no. 1–2, pp. 113–133, Feb. 2009.

[24] D. A. Siegel, T. K. Westberry, M. C. O'Brien, N. B. Nelson, A. F. Michaels, J. R. Morrison *et al.*, "Bio-optical modeling of primary production on regional scales: The Bermuda BioOptics project," *Deep-Sea Res. II*, vol. 48, no. 8–9, pp. 1865–1896, 2001.

[25] M. J. Oliver, O. Schofield, T. Bergmann, S. Glenn, C. Orrico, and M. Moline, "Deriving in situ phytoplankton absorption for bio-optical productivity models in turbid waters," *J. Geophys. Res.: Oceans*, vol. 109, no. C7, pp. 1–12, Jul. 2004, doi: 10.1029/2002JC001627.

[26] H. Claustre, M. Babin, D. Merien, J. Ras, L. Prieur, S. Dallot *et al.*, "Toward a taxon-specific parameterization of bio-optical models of primary production: A case study in the North Atlantic," *J. Geophys. Res.: Oceans*, vol. 110, no. C7, pp. 1–19, Jul. 2005, doi:10.1029/2004JC002634.

[27] J. Marra, C. C. Trees, and J. E. O'Reilly, "Phytoplankton pigment absorption: A strong predictor of primary productivity in the surface ocean," *Deep-Sea Res. I*, vol. 54, no. 2, pp. 155–163, Feb. 2007.

[28] Z. P. Lee, K. L. Carder, J. Marra, R. G. Steward, and M. J. Perry, "Estimating primary production at depth from remote sensing," *Appl. Opt.*, vol. 35, no. 3, pp. 463–474, Jan. 1996.

[29] T. Hirawake, S. Takao, N. Horimoto, T. Ishimaru, Y. Yamaguchi, and M. Fukuchi, "A phytoplankton absorption-based primary productivity model for remote sensing in the Southern Ocean," *Polar Biol.*, vol. 34, no. 2, pp. 291–302, Feb. 2011.

[30] P. J. Werdell, B. A. Franz, S. W. Bailey, G. C. Feldman, E. Boss, V. E. Brando *et al.*, "Generalized ocean color inversion model for retrieving marine inherent optical properties," *Appl. Opt.*, vol. 52, no. 10, pp. 2019–2037, Apr. 2013.

[31] Z. Lee, A. Weidemann, J. Kindle, R. Arnone, K. L. Carder, and C. Davis, "Euphotic zone depth: Its derivation and implication to ocean-color remote sensing," *J. Geophys. Res.: Oceans*, vol. 112, no. C3, pp. 1–12, Mar. 2007, doi: 10.1029/2006JC003802.

[32] H. E. Garcia, R. A. Locarnini, T. P. Boyer, J. I. Antonov, M. M. Zweng, O. K. Baranova *et al.*, "World Ocean Atlas 2009, Volume 4: Nutrients (Phosphate, Nitrate, Silicate)," NOAA Atlas NESDIS 71, U.S. Government Printing Office, Washington, DC, Mar. 2010.

[33] J. Ronald, V. Zaneveld, J. C. Kitchen, and J. L. Mueller, "Vertical structure of productivity and its vertical integration as derived from remotely-sensed observations," *Limnol. Oceanogr.*, vol. 38, no. 7, pp. 1384–1393, Nov. 1993.

[34] T. Platt, C. L. Gallegos, and W. G. Harrison, "Photoinhibition of photosynthesis in natural assemblages of marine-phytoplankton," *J. Mar. Res.*, vol. 38, no. 4, pp. 687–701, 1980.

[35] D. A. Kiefer and B. G. Mitchell, "A simple, steady-state description of phytoplankton growth based on absorption cross-section and quantum efficiency," *Limnol. Oceanogr.*, vol. 28, no. 4, pp. 770–776, 1983.

[36] E. A. Laws, "Photosynthetic quotients, new production and net community production in the open ocean," *Deep-Sea Res. A: Oceanogr. Res. Paper.*, vol. 38, no. 1, pp. 143–167, Jan. 1991.

[37] O. Schofield, B. B. Prezelin, R. R. Bidigare, and R. C. Smith, "In situ photosynthetic quantum yield—Correspondence to hydrographic and optical variability within the Southern California Bight," *Mar. Ecol. Prog. Ser.*, vol. 93, no. 1–2, pp. 25–37, Feb. 1993.

[38] B. Wozniak, D. Ficek, M. Ostrowska, R. Majchrowski, and J. Dera, "Quantum yield of photosynthesis in the Baltic: A new mathematical expression for remote sensing applications," *Oceanologia*, vol. 49, no. 4, pp. 527–542, 2007.

[39] J. S. Cleveland, M. J. Perry, D. A. Kiefer, and M. C. Talbot, "Maximal quantum yield of photosynthesis in the Northwestern Sargasso Sea," *J. Mar. Res.*, vol. 47, no. 4, pp. 869–886, Nov. 1989.

[40] M. Babin, J. C. Therriault, L. Legendre, B. Nieke, R. Reuter, and A. Condal, "Relationship between the maximum quantum yield of carbon fixation and the minimum quantum yield of chlorophyll-a in-vivo fluorescence in the Gulf of St-Lawrence," *Limnol. Oceanogr.*, vol. 40, no. 5, pp. 956–968, Jul. 1995.

[41] J. P. Parkhill, G. Maillet, and J. J. Cullen, "Fluorescence-based maximal quantum yield for PSII as a diagnostic of nutrient stress," *J. Phycol.*, vol. 37, no. 4, pp. 517–529, Aug. 2001.

[42] P. Ricchiazzi, S. R. Yang, C. Gautier, and D. Sowle, "SBDART: A research and teaching software tool for plane-parallel radiative transfer in the Earth's atmosphere," *Bull. Amer. Meteorol. Soc.*, vol. 79, no. 10, pp. 2101–2114, Oct. 1998.

[43] R. W. Austin and T. J. Petzold, "Spectral dependence of the diffuse attenuation coefficient of light in ocean waters," *Opt. Eng.*, vol. 25, no. 3, pp. 471–479, Mar. 1986.

[44] J. Marra, C. Ho, and C. C. Trees, "An alternative algorithm for the calculation of primary productivity from remote sensing data," NASA, LDEO Tech. Rep. 2003-1, 2003.

[45] J. Chen, M. W. Zhang, T. W. Cui, and Z. H. Wen, "A review of some important technical problems in respect of satellite remote sensing of chlorophyll-a concentration in coastal waters," *IEEE J. Sel. Topics Appl. Earth Observ. Remote Sens.*, vol. 6, no. 5, pp. 2275–2289, Oct. 2013.

[46] M. R. Hiscock, V. P. Lance, A. M. Apprill, R. R. Bidigare, Z. I. Johnson, B. G. Mitchell *et al.*, "Photosynthetic maximum quantum yield increases are an essential component of the Southern Ocean phytoplankton response to iron," *PNAS*, vol. 105, no. 12, pp. 4775–4780, Mar. 2008.

[47] S. L. Shang, M. J. Behrenfeld, Z. P. Lee, R. T. O'Malley, G. M. Wei, Y. H. Li *et al.*, "Comparison of primary productivity models in the Southern Ocean: Preliminary results," *Proc. SPIE 7678, Ocean Sens. Monit. II*, 767808, April 20, 2010, doi: 10.1117/12.853631.

[48] N. B. Nelson, D. A. Siegel, and J. A. Yoder, "The spring bloom in the northwestern Sargasso Sea: Spatial extent and relationship with winter mixing," *Deep-Sea Res. II*, vol. 51, no. 10–11, pp. 987–1000, 2004.

[49] H. R. Gordon and D. K. Clark, "Remote-sensing optical-properties of a stratified ocean—An improved interpretation," *Appl. Opt.*, vol. 19, no. 20, pp. 3428–3430, 1980.

[50] Z. P. Lee and K. L. Carder, "Absorption spectrum of phytoplankton pigments derived from hyperspectral remote-sensing reflectance," *Remote Sens. Environ.*, vol. 89, no. 3, pp. 361–368, Feb. 2004.

[51] M. A. Soppa, T. Dinter, B. B. Taylor, and A. Bracher, "Satellite derived euphotic depth in the Southern Ocean: Implications for primary production modelling," *Remote Sens. Environ.*, vol. 137, pp. 198–211, Oct. 2013.

[52] N. B. Nelson, B. B. Prezelin, and R. R. Bidigare, "Phytoplankton light-absorption and the package effect in California Coastal Waters," *Mar. Ecol. Prog. Ser.*, vol. 94, no. 3, pp. 217–227, Apr. 1993.

[53] T. Hirata, J. Aiken, N. Hardman-Mountford, T. J. Smyth, and R. G. Barlow, "An absorption model to determine phytoplankton size classes from satellite ocean colour," *Remote Sens. Environ.*, vol. 112, no. 6, pp. 3153–3159, Jun. 2008.

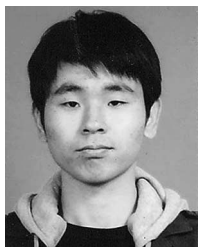

Sheng Ma received the B.S. degree in resources science and technology from Beijing Normal University, Beijing, China, in 2009. He is currently pursuing the Ph.D. degree in cartography and geographic information system from Institute of Remote Sensing and Digital Earth (RADI), Chinese Academy of Sciences (CAS), Beijing, China.

His research interests include satellite oceanography, optical image processing, and marine ecological studies.

Zui Tao was born in China, in 1984. He received the B.S. degree in cartography and geographic information system from Henan University, Kaifeng, China, in 2005, the M.S. degree in cartography and geographic information system from Wuhan University, Wuhan, China, in 2008, and the Ph.D. degree in cartography and geographic information system from Institute of Remote Sensing and Digital Earth (RADI), Chinese Academy of Sciences (CAS), Beijing, China, in 2012.

He is currently a Research Associate in RADI, CAS. His research interests include ocean color remote sensing, optical image processing, and marine environmental monitoring.

Xiaofeng Yang (S'07–M'11) received the B.S. degree in environment science from Sichuan University, Chengdu, China, in 2005, and the Ph.D. degree in cartography and geographic information system from the Institute of Remote Sensing Applications (IRSA), Chinese Academy of Sciences (CAS), Beijing, China, in 2010.

During his Ph.D. program, in 2009–2010, he was a Visiting Research Scientist with the Department of Atmospheric and Oceanic Science, University of Maryland, College Park, MD, USA. From 2010 to 2012, he was an Assistant Researcher in IRSA/CAS. Since 2013, he has been with RADI, CAS as an Associate Researcher. His research interests include satellite oceanography, synthetic aperture radar image processing, and marine atmospheric boundary layer process studies. He has also participated in developing various types of operational ocean products in China coastal waters from environmental satellite data.

Dr. Yang has also served as a reviewer of several international academic journals.

Yang Yu received the B.S. degree in cartography and geographic information system from Shanghai Institute of Technology, Shanghai, China, in 2005, and the M.S. degree in physical oceanography from First Institute of Oceanography (FIO), State Oceanic Administration People's Republic of China (SOA), Qingdao, China, in 2010. She is currently pursuing the Ph.D. degree in cartography and geographic information system from Institute of Remote Sensing and Digital Earth (RADI), Chinese Academy of Sciences (CAS), Beijing, China.

She is currently a Research Associate in RADI, CSA. Her research interests include marine dynamics and marine environmental monitoring.

Xuan Zhou received the Ph.D. degree in cartography and geographic information system from the Institute of Remote Sensing and Digital Earth (RADI), Chinese Academy of Sciences (CAS), Beijing, China, in 2012.

His research interests include satellite oceanography, typhoon observation, and radar remote sensing.

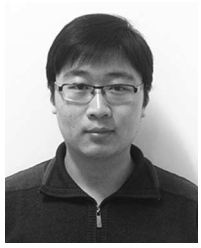

Wentao Ma received the B.S. degree from Ocean University of China (OUC), Qingdao, China, in 2010. He is currently pursuing the Ph.D. degree in physical oceanography and ocean remote sensing from College of physical and Environmental Oceanography (CPEO), OUC.

His main research fields are satellite oceanography, algorithms for microwave radiometer, and salinity remote sensing.

Ziwei Li received the B.S. and M.S. degrees in photogrammetry and remote sensing from the People's Liberation Army (PLA) Information Engineering University, Zhengzhou, China, in 1982 and 1990, respectively.

She was an Assistant Professor with the Department of Geomatics, PLA Information Engineering University, before joining the Chinese Academy of Surveying and Mapping, Beijing, China, in 1996. From 2006 to 2007, she was a Research Fellow with First Institute of Oceanography, State Oceanic Administration of China, Qingdao, China. Since 2008, she has been with the Institute of Remote Sensing and Digital Earth (RADI), Chinese Academy of Sciences (CAS), Beijing, China. Her research has focused on the application of remote sensing data for oceanography and meteorology studies.